JOURNAL OF BACTERIOLOGY, June 1976, p. 1278-1284
Vol. 126, No. 3
Copyright © 1976 American Society for Microbiology
Printed in U.S.A.

Ultrastructure of *Polyangium cellulosum*

J. R. LAMPKY

Department of Biology, Central Michigan University, Mt. Pleasant, Michigan 48859

Received for publication 16 March 1976

Polyangium cellulosum was examined with the transmission electron microscope and the scanning electron microscope. Freeze-fracturing and critical-point-drying techniques were employed with the latter instrument. Critical-point drying seemed to eliminate the distortion of cells and fruiting bodies. These instruments and techniques allowed for a detailed comparison of cell and fruiting-body ultrastructure. Lipid storage materials and mesosomes were found to be constant cell particulates in both vegetative cells and in the shortened myxospores.

In the last 20 years, electron microscopy has provided an understanding of the fine structure of selected fruiting myxobacterial species. However, this information was obtained with the transmission electron microscope (TEM) exclusively (1-3, 5, 7, 8, 10, 13, 15, 16, 17-19). Jackson and Peterson (Bacteriol. Proc., p. 38, 1969) described some of the ultrastructure of *Polyangium cellulosum* (*Sorangium cellulosum*).

More recently, scanning electron microscopy (SEM) studies (4, 9, 14) have shown some details of the exterior of individual cells and fruiting bodies. Each of the studies has contributed to our relatively meager knowledge of the fine structure of fruiting myxobacteria.

The electron microscope studies have, for the most part, dealt with fruiting myxobacterial genera other than *Polyangium*. Moreover, relatively few studies have used both TEM and SEM to compare myxobacterial vegetative cells and fruiting bodies from sectioned material and whole mounts. It was the purpose of this study to correlate the fine structure of the cellulolytic fruiting myxobacterium *P. cellulosum* Imshenetski, Solntseva, and Peterson, as observed with the TEM and SEM, and utilizing freeze fracturing and critical-point drying with the latter.

MATERIALS AND METHODS

Organism. The strain of *P. cellulosum* used in this study was originally isolated from Missouri soils in 1961. Since that time, it has been stored in a soil-solka floc mixture in a screw-capped jar at room temperature (20 to 30 C). The bacteria-soil-solka floc mixture has become rather dry over the period of 14 years.

Cultivation. Cells for electron microscopy were grown on an inorganic salts agar medium consisting of 0.75 g of KNO_3, 0.75 g of K_2HPO_4, 0.15 g of $MgSO_4 \cdot 7\ H_2O$, 0.02 g of $CaCl_2$, 0.015 g of $FeCl_3$, 15.0 g of agar, and 1.0 liter of distilled water. Following sterilization and cooling, the agar was poured into sterile disposable culture plates. Sterile Whatman no. 1 filter paper strips were placed on the cooled agar surface. The filter paper served as the sole carbon source for the bacteria.

A small pile of the bacteria-soil-solka floc was placed at the center of the filter paper strip with a sterile spatula. The plates were inverted and incubated at room temperature for 2 to 3 weeks.

Fixation and microscopy. For TEM, the organism on the agar surface was flooded with 0.1% Veronal-acetate-buffered OsO_4, pH 6.8, for 0.5 h at room temperature (ca. 22 C). The cells and fruiting bodies were gently scraped from the agar surface with a razor blade and rinsed into a vial with 1.0% Veronal-acetate-buffered OsO_4, pH 6.8, for 16 h at room temperature. Following fixation, the cells and fruiting bodies were rinsed in 0.5% (wt/vol) uranyl acetate in the Veronal-acetate buffer for 2 h. The cells and fruiting bodies were finally rinsed for 20 min in the buffer solution alone.

The myxobacterium was dehydrated through an acetone series, embedded in Mollenhauer mixture no. 1 (10), and sectioned on a Porter-Blum MT-2 ultramicrotome using a glass knife. Sections were stained for 15 min with a 2.0% uranyl acetate in 50% ethanol, pH 4.0, and with lead citrate (12) for 7 min; observations were made using a Phillips 300 electron microscope operating at 60 kV.

Two percent glutaraldehyde was used as the fixative for SEM studies of both vegetative cells and fruiting bodies. The plates upon which the organism grew were flooded with the fixative for 12 to 24 h before SEM observations. Selected squares of agar were cut out from the plates and were subjected to critical-point drying using CO_2 as the carrier gas for approximately 30 min. The dried squares were then glued onto aluminum stubs and coated with gold-palladium alloy (60:40) in a Film-Vac Mini-coater evaporator. The myxobacteria were then examined on an AMR 900 scanning microscope operated at 21 kV.

For freeze-fractured observations, squares that had been fixed as above were frozen in an ethanol-

dry ice mixture for 10 min. The frozen squares were placed on paper toweling and were struck sharply with a scapel to fracture the fruiting bodies. The fractured portions were critically point dried, attached to stubs, coated, and examined as described above.

RESULTS

Organism storage and recovery. Findings in this work indicated that myxobacteria cells of *P. cellulosum* were viable after a rather long period of storage. Myxobacterial growth on the filter paper was at first yellow, which changed to brown as fruiting bodies matured. Slime-veined swarms fanned out over the agar surface. The swarm on the agar was colorless at first, but turned brown as sori formed. Cell growth and fruiting-body formation appeared to be equally as good as was observed 14 years previously.

Fine structure. Figure 1, a TEM thin section, illustrates a young *P. cellulosum* vegetative cell. It has a typical gram-negative cell wall, peptidoglycan layer, and unit membrane. Several vesicular mesosomes are present between the cell membrane and the peptidoglycan layer. Sudanophilic, malachite green-positive, single-membrane inclusions are observed at each end of the cell. Within the cytoplasm is a mixture of fibrillar nuclear material with abundant ribosomes or ribosomal masses. Exterior to the cell are unit membrane vesicles, appearing similar to those within the mesosomes.

An SEM micrograph (Fig. 2) also shows a young vegetative cell that has fibrous extensions attached to its exterior. Particular attention should be drawn to the similarities between the extensions and the vesicles noted in Fig. 1.

As the cells begin to approach the time of aggregation, the cell wall (Fig. 3) begins to take on a wavy appearance. All other cell particulates seem to remain similar in appearance to those noted in the young vegetative cell.

Figures 4 and 5 are TEM and SEM micrographs, respectively, showing typical shorter cells just prior to becoming a myxospore. The cellular inclusions mentioned earlier are clearly evident.

The TEM thin sections (Fig. 6 and 7) of a sporangium show myxospores. The cytoplasmic materials have been considerably compressed and distorted. Mesosomes are evident in the myxospores contained within the sporangium (see arrow). Spherical unit membrane vesicles are still observed around and between the cells. The individual myxospores appear to lack definite capsules.

An SEM photograph (Fig. 8) illustrates a freeze-fractured sporangium containing short myxospores. The outer covering is the slime coat of the sporangium. In the lower portion of the photograph there are no cells present; it is thought that the holes were the location of myxospores prior to freeze fracturing.

Figure 9 is a TEM thin-section photograph of a cell in a fibullar track furrow in which the myxobacterial cell moves.

Slime production by *P. cellulosum* is depicted in Fig. 10. The myxobacterial cells are shown attached to a cellulose fiber. At a later stage, cells are shown on another cellulose fiber (Fig. 11) upon which ridges and valleys of slime appear to coat the fiber. Clearly the cells move along the valleys; such is the case in Fig. 9 and 11.

Development of a sorus consisting of many sporangia begins with the massing or aggregation and heaping-up of *P. cellulosum* cells (Fig. 12). Within several days, sporangia begin to delineate as the slime encompasses smaller cell masses (Fig. 13).

Figure 14 is an SEM photomicrograph of a sorus consisting of numerous sporangia. Each sporangium within the sorus contains numerous myxospores. A freeze-fractured sorus illustrates the polygonal shape of the sporangia (Fig. 15).

DISCUSSION

The recovery of many myxobacterial species after prolonged storage has, in the past, generally met with little success. The method for storage used here was a mixture of cell-soil-solka floc, and it appeared to be a means of successfully maintaining this strain of *P. cellulosum*. Recovery of this strain of myxobacterium was 100% successful on the inorganic salts agar medium.

Several interesting and significant differences by TEM and SEM from other fruiting myxobacterial species appear to have been shown in this work. Although the findings seem to be true differences from other species, it is not impossible that the specimen preparation was adequately different from other studies. The differences in preparation may explain why some cell particulates were not shown in other work.

The sudanophilic, malachite green-positive inclusions are indicative of a lipid storage material as suggested by McCurdy (8). These inclusions appear to have a single outer covering, unlike other cell inclusions, which are normally bound by a unit membrane.

Abadie (1) noted that mesosomes disappeared

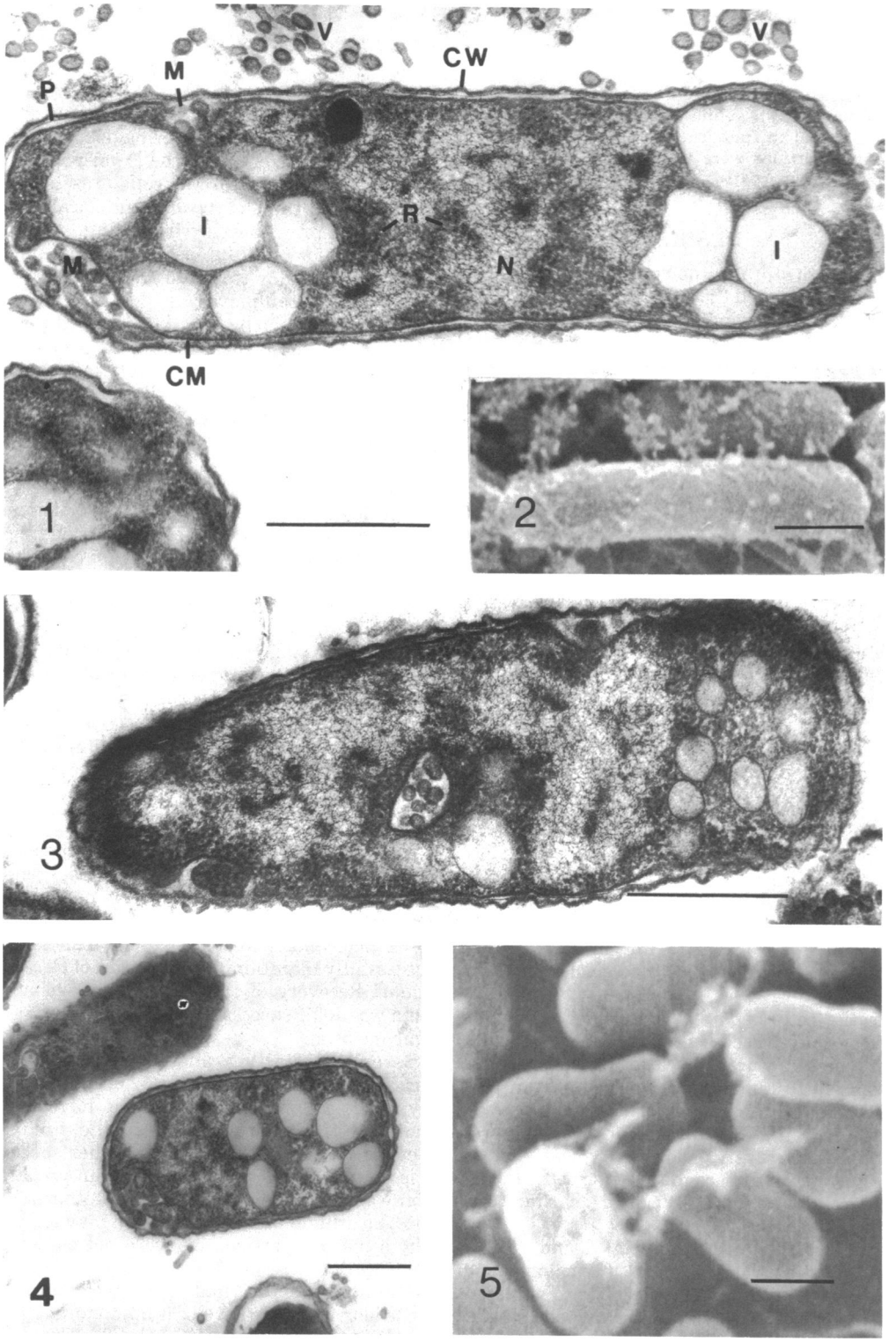

FIG. 1. *Thin section of a young vegetative cell showing the cell wall (CW), peptidoglycan layer (P), cell membrane (CM), inclusion (I), nuclear material (N) ribosomes (R), mesosomes (M), and vesicles (V). Bar is 0.5 μm.*

FIG. 2. *SEM micrograph of a young vegetative cell with fibrous extensions. Bar is 1.0 μm.*

FIG. 3. *Thin-sectioned older cell; note the wavy appearance of the cell wall. Bar is 0.5 μm.*

FIG. 4. *Sectioned, shortened older cell just prior to myxospore formation. Bar is 0.5 μm.*

FIG. 5. *An SEM photograph of cells prior to forming myxospores. Bar is 0.5 μm.*

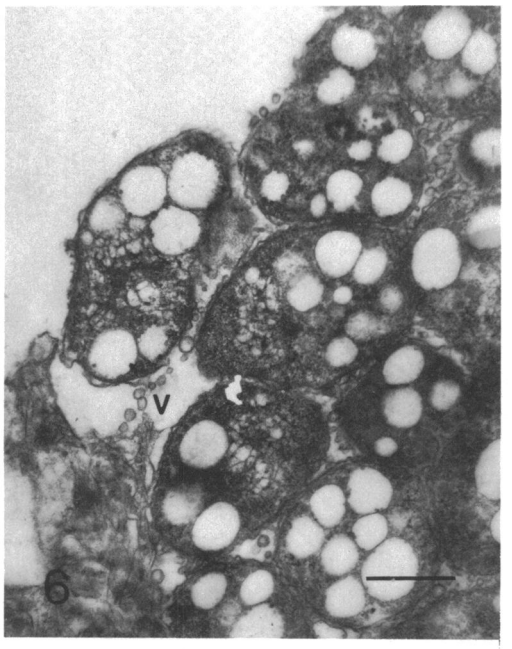

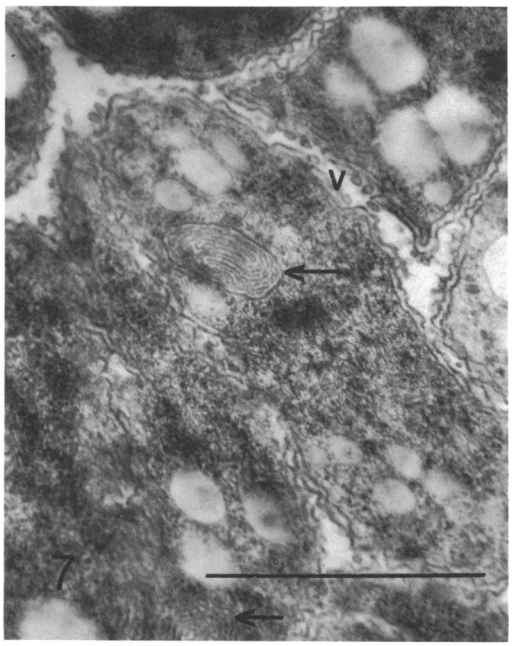

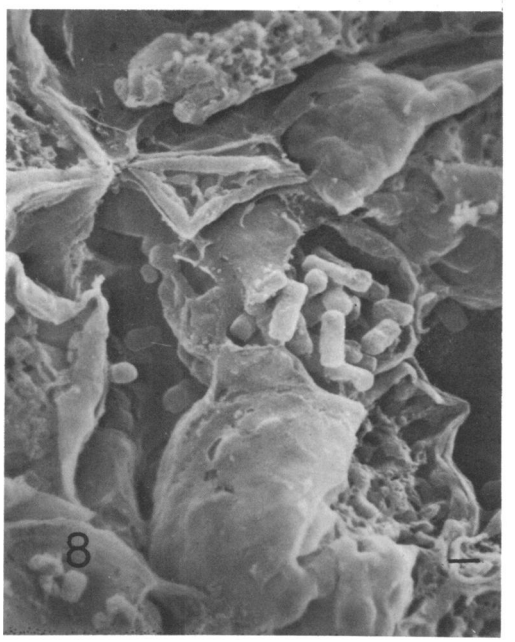

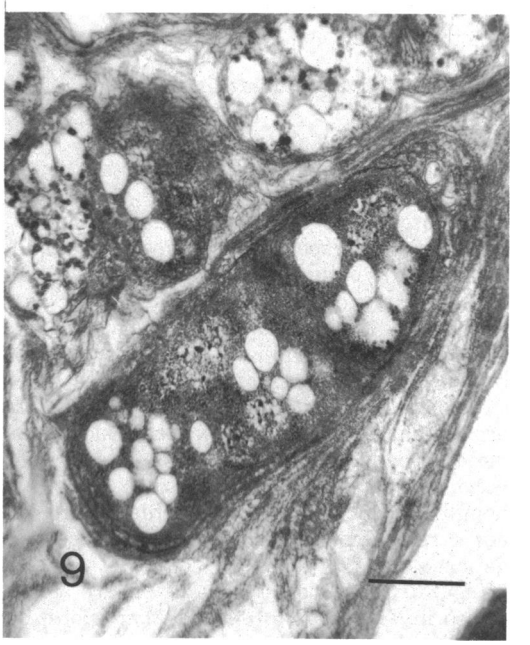

FIG. 6 and 7. *Sectioned myxospores in a sporangium; although the cellular components are compressed, individual particulates are evident including mesosomes (arrows) and extracellular vesicles (V). Fig. 6, bar is 0.5 μm; Fig. 7, bar is 0.5 μm.*

FIG. 8. *A freeze-fractured sporangium as viewed with SEM. The myxospores remain in place above center, where in the lower right depressions indicate myxospore removal. Bar is 1.0 μm.*

FIG. 9. *A fibrillar slime furrow is evident on either side of the sectioned vegetative cell. Bar is 0.5 μm.*

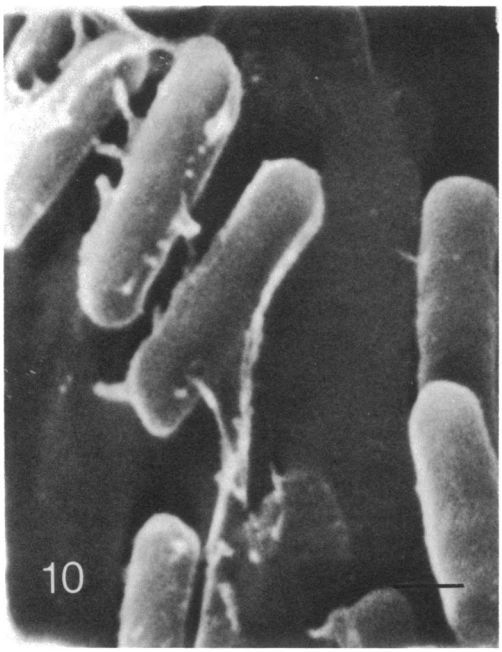

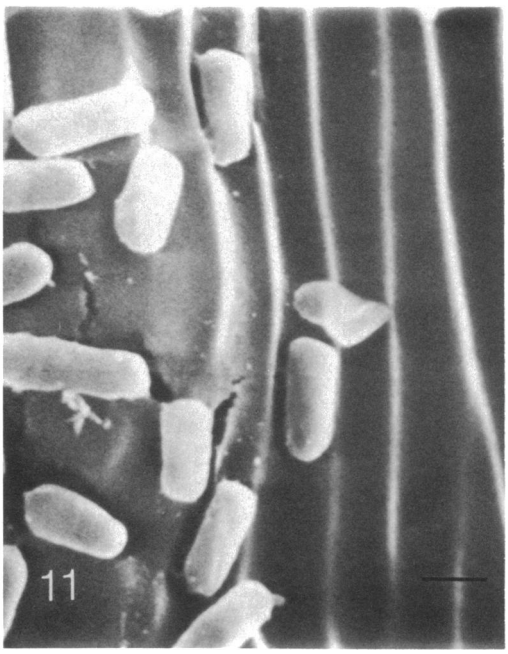

FIG. 10. *Vegetative cells are attached to a cellulose fiber. Note the slime strands extending from the cells. Bar is 0.5 μm.*

FIG. 11. *At a later stage, the vegetative cells move along the valley portion of the furrow. Bar is 1.0 μm.*

during the latent life phase of *Chondromyces crocatus*. It would appear that *P. cellulosum* myxospores differ from the myxospores of *C. crocatus* in this aspect. Mesosomes in this cellulolytic species occur in both the vegetative cells and in the myxospore resting stage.

This work concurs, in part, with the findings of Schmidt-Lorenz (13). Fibrous extensions or threadlike protrusions as illustrated by SEM photomicrographs extend outward into the external environment as a network. Vesicles surrounding cells in TEM micrographs represent sections of what is interpreted to be slime. Although not conclusively shown, this may represent a release of bacterial waste products via the mesosomes.

Vegetative cells of *P. cellulosum* are as described in *Bergey's Manual* (6). Myxospores do resemble the vegetative cells in shape, but not in size; the myxospores are considerably shorter in length. In addition, the cell wall and cell membrane of the myxospore differ from those of the vegetative cell in that the myxospores develop irregular waves; the vegetative cell wall and cell membrane are relatively free of irregular waves. Myxospores within a sporangium become compressed or distorted in shape from what appears to be an irregular, haphazard cell arrangement and mutually induced pressure.

Previous studies (4, 9, 14) have used air-dried specimens; air drying seems to cause stress upon, at least, the fruiting-body structures, and perhaps demonstration of the slime protrusions from vegetative cells.

The findings in this work suggest that air drying of specimens imposes a more than necessary physical distortion, and hence, does not provide a complete and true picture of organisms viewed by SEM. It seems that critical-point drying may very well be one means of better preserving morphological integrity, thereby permitting the investigator to make a more accurate assessment of the material observed.

Initiation of the sporangia and eventually of the sorus takes place when partially shortened cells begin to accumulate and heap-up into a mass. Considerable amounts of slime occur at the surface and internally between sporangia. At this time a number of myxospores begin to be encompassed in a more-or-less spherical mass, the sorus, and several to many sporangia which are accumulated are held together by slime.

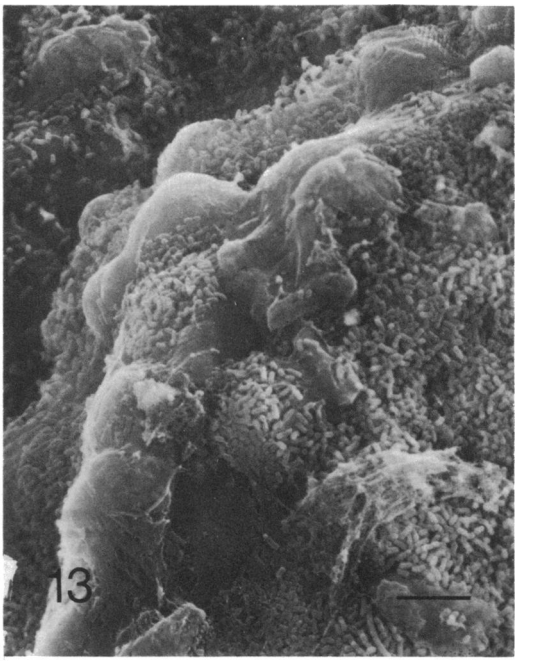

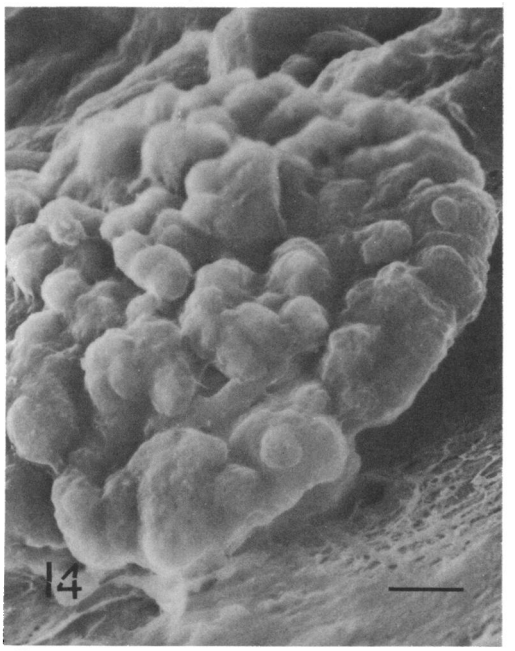

FIG. 12. *Cell aggregation and heaping-up prior to sporangia and sorus formation.*
FIG. 13. *Slime encompassing cell masses to form sporangia.*
FIG. 14. *A number of sporangia constitute a sorus.*
FIG. 15. *A freeze-fractured sorus illustrating the polygonal forms of the sporangia. Fig. 12–15, bar is 5.0 μm.*

ACKNOWLEDGMENTS

I thank J. D. Adams, E. R. Brockman, L. D. Koehler, and D. E. Wujek for their constructive comments during the preparation of this manuscript. I also wish to thank Larry Tait and Art Ackerson for their electron microscopy technical assistance.

This research was supported by the Research and Creative Endeavors Committee of Central Michigan University.

LITERATURE CITED

1. **Abadie, M.** 1967. Intracytoplasmic formations of the "mesosome" in *Chondromyces crocatus* Berkley and Curtis. C. R. Acad. Sci. Ser. D 265:2132-2134.
2. **Abadie, M.** 1968. Evidence of mesosomic formation in the vegetative cells of *Chondromyces apiculatus* Thaxter. C. R. Acad. Sci. Ser. D 267:1538-1540.
3. **Bacon, K., and F. A. Eiserling.** 1968. A unique structure in microcysts of *Myxococcus xanthus*. J. Ultrastruct. Res. 21:378-382.
4. **Brockman, E. R., and R. L. Todd.** 1974. Fruiting myxobacters as viewed with a scanning electron microscope. Int. J. Syst. Bacteriol. 24:118-124.
5. **Burchard, R. P., and D. T. Brown.** 1973. Surface structure of gliding bacteria after freeze-etching. J. Bacteriol. 114:1351-1355.
6. **Buchanan, R. E., and N. E. Gibbons (ed.).** 1974. Bergey's manual of determinative bacteriology, 8th ed. The Williams & Wilkins Co., Baltimore.
7. **Kühlwein, J.** 1969. Some aspects of morphogenesis and fruiting body formation in myxobacteria. J. Appl. Bacteriol. 32:19-21.
8. **McCurdy, H. D., Jr.** 1969. Light and electron microscope studies of the fruiting bodies of *Chondromyces crocatus*. Arch. Mikrobiol. 63:380-390.
9. **McNeil, K. E., and V. B. D. Skerman.** 1972. Examination of myxobacteria by scanning electron microscopy. Int. J. Syst. Bacteriol. 22:243-250.
10. **Mollenhauer, H. H.** 1964. Plastic embedding mixtures in electron microscopy. Stain Technol. 39:111-114.
11. **Reichenbach, H., H. Voelz, and M. Dworkin.** 1969. Structural changes in *Stigmatella aurantica* during myxospore induction. J. Bacteriol. 97:905-911.
12. **Reynolds, E. S.** 1963. The use of lead citrate at high pH as an electron-opaque stain in electron microscopy. J. Cell Biol. 17:208.
13. **Schmidt-Lorenz, W.** 1969. The fine structure of the swarm cells of myxobacteria. J. Appl. Bacteriol. 32:22-23.
14. **Shimkets, L. and T. W. Seale.** 1975. Fruiting-body formation and myxospore differentiation and germination in *Myxococcus xanthus* viewed by scanning electron microscopy. J. Bacteriol. 121:711-720.
15. **Voelz, H.** 1965. Formation and structure of mesosomes in *Myxococcus xanthus*. Arch. Mikrobiol. 51:60-70.
16. **Voelz, H.** 1967. The physical organization of the cytoplasm in *M. xanthus* and the fine structure of its components. Arch. Mikrobiol. 57:181-195.
17. **Voelz, H., and M. Dworkin.** 1962. Fine structure of *Myxococcus xanthus* during morphogenesis. J. Bacteriol. 84:943-952.
18. **Voelz, H. and H. Reichenbach.** 1969. Fine structure of fruiting bodies of *Stigmatella aurantica* (myxobacterales). J. Bacteriol. 99:856-866.
19. **Zhilina, T. N.** 1968. Fine structure of the myxobacterium *Archangium sp.* Mikrobiologiya 37:903-907.